The effects of soil density on the response of a bridge with soil-foundation-structure-interaction under near-fault earthquake: experimental investigation

2015 NZSEE
Conference

D. Pradhan, T. Sibaev, Y. Chen & T. Larkin

Department of Civil and Environmental Engineering, the University of Auckland, Auckland

ABSTRACT: In conventional design of bridge piers, the superstructure is sometimes assumed to be fixed at the base and nonlinear soil deformation under the foundation is not considered. Recent studies have suggested that this philosophy sometimes results in a conservative design of both the foundation and the superstructure. Considering soil-foundation-structure-interaction (SFSI) may make the overall design of the structure-foundation system less conservative and more economical. Evidence has been found that the near-fault ground motions with enhanced acceleration pulses can result in a higher demand on the structure compared to far-field earthquakes. However, the number of experimental investigations on SFSI under near-fault earthquake motion is limited. Hence, in this study shake table tests on a scaled bridge pier model were conducted. The foundation of the model was designed to allow SFSI to occur since the supporting medium was sand. The effects of varying soil density were considered. A pressure mat was placed to measure the pressure distribution at the foundation-soil interface. Both near-fault and far-field ground motions were utilised. The results show that during near-fault ground motion, the dominant frequency of the induced vibration of the bridge pier reduces with deceasing relative density of the soil. However, this is not observed when the model is subjected to far-field ground motion. The results also show that the maximum contact pressure on the foundation reduces with the decrease in relative density.

1 INTRODUCTION

Near field earthquake ground motions have been found to have different characteristics to those in the far-field (Anderson and Bertero 1987; Chopra 2001). One of the important characteristics is energy often becomes concentrated in a long period acceleration pulse (Somerville 1997). Structures experience large deformation in only a few cycles of motion. However, structures undergo small deformations in a large number of cycles when subjected to far-field earthquakes (Anderson and Bertero 1987).

In the New Zealand Loadings Standard, NZS 1170.5 (2004), a near-fault factor (*N[T,D]*) is adapted to implement the effect of near-fault ground motions. This, however, has proven to be inaccurate to represent the effects of the 2010 Darfield earthquake. Even with the maximum near-fault factor applied, spectral accelerations of the recorded ground motions far exceeded NZS 1170.5:2004 prescribed values (Bradley 2012). Some structures on shallow foundations have performed extremely well during this earthquake. Through post-earthquake investigations, this was linked to soil-foundation-structure interaction (SFSI). A large portion of seismic energy was dissipated through plastic action of the underlying soil and partial uplift of the foundation (Storie et al. 2014). Rodriguez and Montes (2000) have also evaluated the importance of SFSI effects on the seismic response of buildings and foundations in Mexico City during the 1985 earthquake. Study of Trifunac and Todoroska (1999) has attempted to quantify the effects of soil strain, structural properties and the intensity of the shaking on the response of structures with SFSI during the 1994 Northridge earthquake. The results of this numerical study indicated that the number of severely damaged buildings was reduced in areas where strain in soil was low.

A limited number of experimental studies have considered energy dissipation and SFSI (Qin et al. 2013; Chen et al. 2013). However, in most of these investigations the effect of large acceleration pulses was not taken into account nor was the effect of soil density. Therefore, in this study soil-foundation-structure interaction of a bridge pier subjected to near-fault ground motion with acceleration pulse was investigated. Particular interest is taken in the effects of soil density on the pressure distribution at the foundation-soil interface.

2 METHODOLOGY

2.1 Prototype

The bridge pier prototype was designed to have a shallow, rectangular foundation. The prototype consisted of a 121.5 tonne mass, supported by a 9 m height column with EI = 7807x10^6 kNm^2. This resulted in a natural frequency (f_p) of 2.59 Hz.

The equivalent static method was utilised to assess the seismic action in accordance with NZS1170.5:2004 for a Christchurch site, subsoil class D, assuming annual probability of exceedance (APE) of 1/1000. The foundation of the pier was designed using Verification Method B1/VM4 in the New Zealand Building Code (DBH, 2011) for shallow foundations. The adopted dimensions were 8.4m long by 2.25m wide by 1.3m thick. A factor of safety of 1 for the seismic design of the foundation was adopted.

2.2 Model

The prototype was represented as a single degree of freedom system and downscaled using the principles of similitude, according to the dimensionless groups outlined in Drosos et al. (2012) for geotechnical applications. The scale factors are shown in Table 1.

Table 1. Dimensionless scale factors applied.

Length	$S_L = 15$
Mass	$S_m = S_L^3 = 3375$
Acceleration	S_a=1
Time	$S_t = \sqrt{S_L/S_a} = 3.873$
Lateral Stiffness	$S_k = \frac{S_a * S_m}{S_L} = 225$

The model was constructed from steel and the ratio of ultimate bearing capacity to applied vertical load was equal in both the prototype and the model. Table 2 provides the summary of the key model dimensions. Figure 1 illustrates the model used in the study.

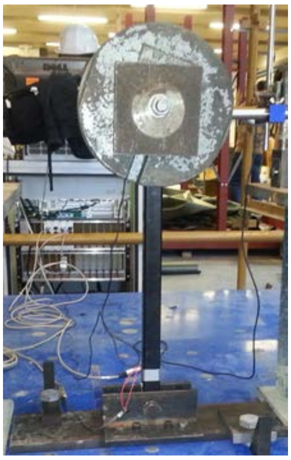

Figure 1. SDOF model.

Table 2. Properties of the model.

Effective Height	600mm
Mass on Top	36kg
Column	35x35x3mm SHS
Foundation	150x560x12mm
Natural frequency (f_m)	10 Hz

2.3 Ground Motions

The ground motions used in the experiments are presented in Figure 2. The ground motion component, N64W, recorded at the Christchurch Cathedral College (CCCC) station (R_{rup} = 2.8 km) from the 2011 Christchurch earthquake was chosen to represent the near-fault motion which contained a pronounced acceleration pulse (highlighted in Figure 2(a); GeoNet, (2011)). The far-field ground motion was stochastically generated based on the design spectrum specified in NZS1170.5:2004 for subsoil class D, using the method described by Li et al. (2012). Both ground motions were scaled to match the target spectrum (site class D in Christchurch with a return period of 1000 years) between the periods of 0.4T and 1.3T, where T is the fundamental period, using the method described in NZS 1170.5. The time scaling factor in Table 1 was applied to both ground motions to preserve similitude in the shake table testing. The spectrum acceleration of the applied CCCC motion is larger than that of the NZS motion for the long periods i.e. from 0.12 to 0.52 s, as shown in Figure 2(c).

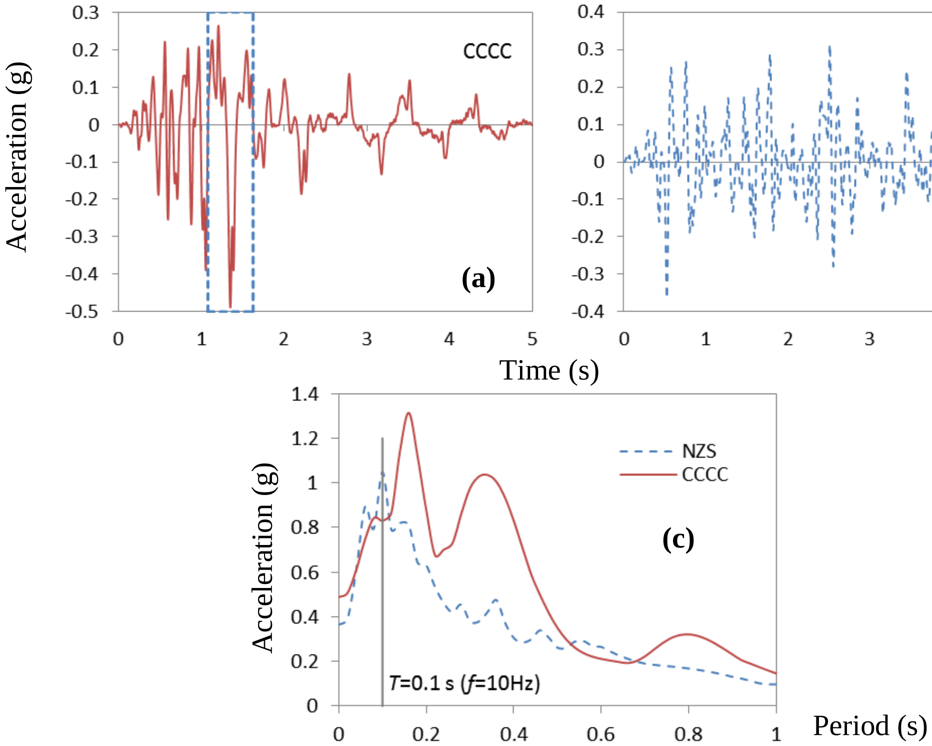

Figure 2. (a) CCCC, (b) NZS ground motions applied and (c) their spectra (5%).

2.4 Sand deposition, properties and testing procedure

The sand was placed in a laminar box, constructed to approximately simulate shear deformation of the sand as it occurs in situ, using a similar procedure to Qin et al. (2013). The sand was rained from a height of 0.9m above the shake table through the floor of a box containing holes at constant spacing. To ensure the density of the sand was uniform spatially, samples were taken during raining of the sand at various locations in the laminar box. The dry density was measured to be on average 15.3 kN/m^3. The relative density was measured in accordance with NZS 4402.4.2 (1988) to be on average 35%, i.e. loose sand according to NZGS (2005). A summary of the test results is given in Table 4.

The particle size distribution (Cheung et al, 2013) indicated that the sand was free from any fines (i.e. < 0.001mm). This suggested that the sample was clean sand and could be compacted readily under dry conditions. A sequence of shake table tests was performed for each ground motion. Since each test compacted the soil, results were achieved for a range of densities. Testing continued for each ground motion until the soil was compacted to the maximum achievable density, i.e. no further settlement due to shaking occurred. The relative density following compaction was estimated to be approximately 90% according to the measured final settlement. The sample at this density was classified as dense sand.

Table 4. Sand properties pre-compaction.

Sand Bulk Density, γ	15.2-15.5 kN/m^3
Relative Density	33%-47%
Soil Friction Angle , ϕ	37°

The shake table testing was performed for three base conditions: i) fixed base, ii) free to uplift on a rigid base and iii) free to uplift on a base of sand. A 300kN capacity, single axis shake table was used for the testing. The fixed base assumption was simulated by fixing the foundation of the model to the shake table using clamps (Figure 3(a)). For the second base condition the clamps were removed and the model was placed on the shake table without any constraint. For final base condition the intent was to simulate SFSI. The setup for the SFSI test is shown in Figure 3(b). The sand was deposited by raining at the beginning of testing for each ground motion. After each test of the sequence, as described above, the sand was smoothed and levelled and the model re-placed on the surface of the sand.

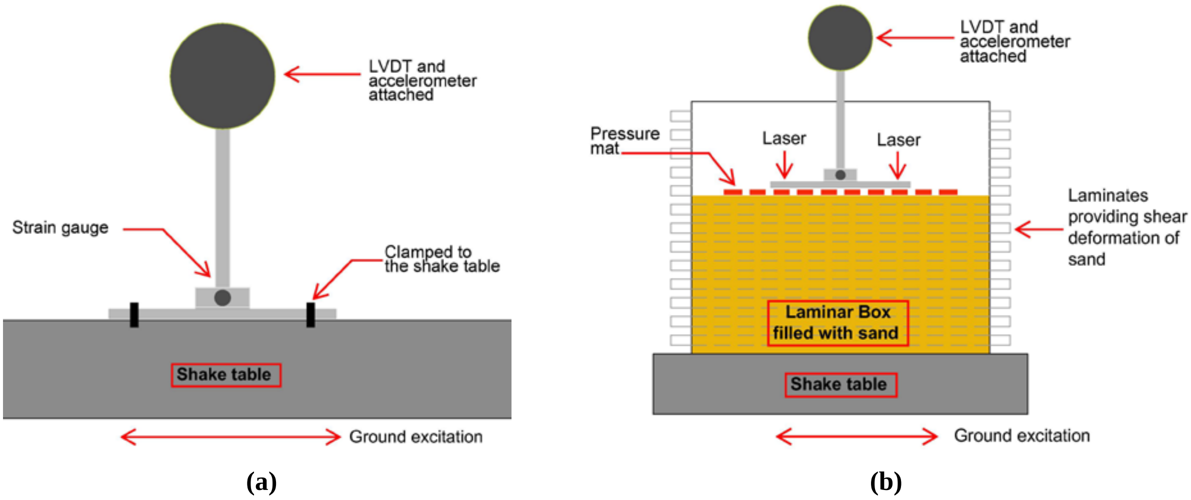

Figure 3. Experimental setup for (a) model fixed on rigid base and (b) with SFSI.

3 RESULTS AND DISCUSSION

3.1 Comparison of shake table results when using recorded near-fault and NZS simulated motions

The maximum displacement induced at the top of the model was compared for all base conditions. It can be seen from Figure 4 that fixed and free on the rigid base conditions produce very similar maximum displacements at the top of the model under both ground motions. However, when SFSI is considered, CCCC motion causes a much higher maximum displacement. This indicates that the strong acceleration pulse significantly increase the deformation of the sand compared with that measured using a stochastic motion.

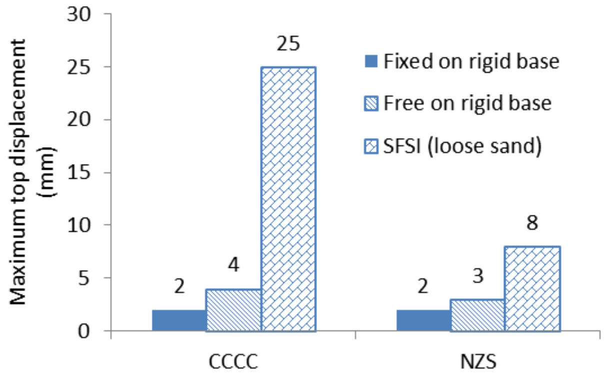

Figure 4. Maximum displacement at the top of the model for two motions.

3.2 Effect of different sand density

The effect of base conditions on the acceleration of the top of the model under the NZS motion is shown in Figure 5(a). The spectra of the accelerations at the top of the model show a decrease in dominant frequency from 10 Hz to 8.3 Hz when comparing fixed base to free on a rigid base condition. A further decrease from 8.3 Hz to 5 Hz can be seen when sand is considered. However, there is no difference in the dominant frequency between the cases on dense and loose sand. This means that the change in sand density has no significant effect on dominant frequency of the accelerations induced by NZS simulated ground motion.

In the case of the model placed on sand and subjected to the CCCC motion, it can be seen that the dominant frequency decreases from 5 Hz for dense sand to 2.9 Hz for loose sand, see Figure 5(b). This suggests that the strong acceleration pulse has a significant influence on the induced acceleration of a model with SFSI.

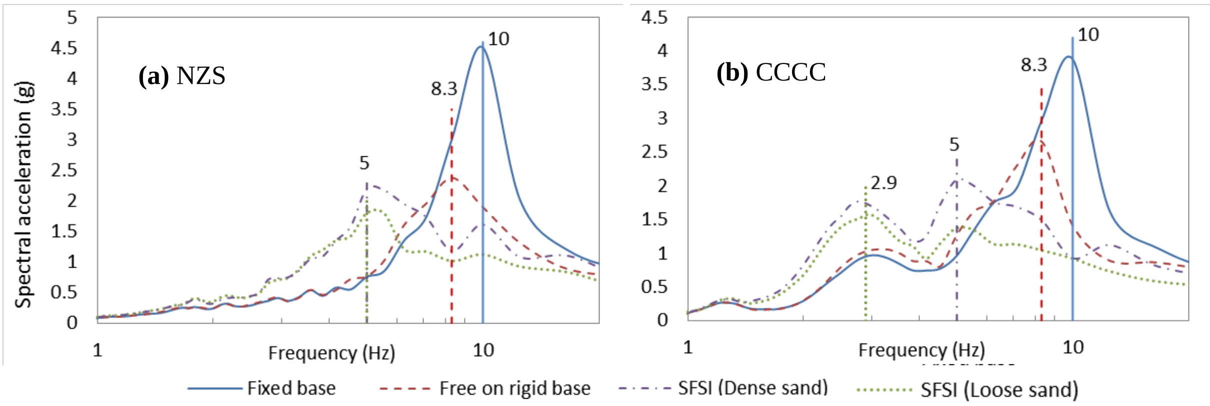

Figure 5. Response spectra (5%) of (a) NZS and (b) CCCC induced accelerations at the top of the model.

3.3 The normal pressure distribution at the foundation-soil interface

The pressure distribution at the foundation-soil interface was recorded using the Tactile pressure mapping system. A matrix of 7x30 sensors points was utilised. The authors recognise that placing a pressure mat in the experimental system has the potential to create inaccuracies, however, the accuracy of this system to reliably measure normal pressure was confirmed by Palmer et al. (2009). The soft sensor pad is designed to conform to any complex, contoured and deformable support surface. Figure 6 summaries the pressure mat readings during the CCCC ground motion. At the time of the strong acceleration pulse (point 1, Fig. 6(a)), uplift of the foundation occurs, as shown by the sharp reduction in contact area (Fig. 6(b). The maximum pressure reading on the dense sand is significantly higher than that on the loose sand, see Figure 6(a). However, referring to the contact area at the time of the strong acceleration pulse, both dense and loose sand conditions resulted in a very similar foundation contact area (Fig. 6(b)).

Figure 7 shows the details of the pressure distribution along with a schematic sketch showing the location of the foundation during uplift. It indicates that for dense soil the seismic forces are predominantly dissipated through foundation uplift. For loose soils, on the other hand, plastic deformation becomes a more dominant mode of seismic energy dissipation.

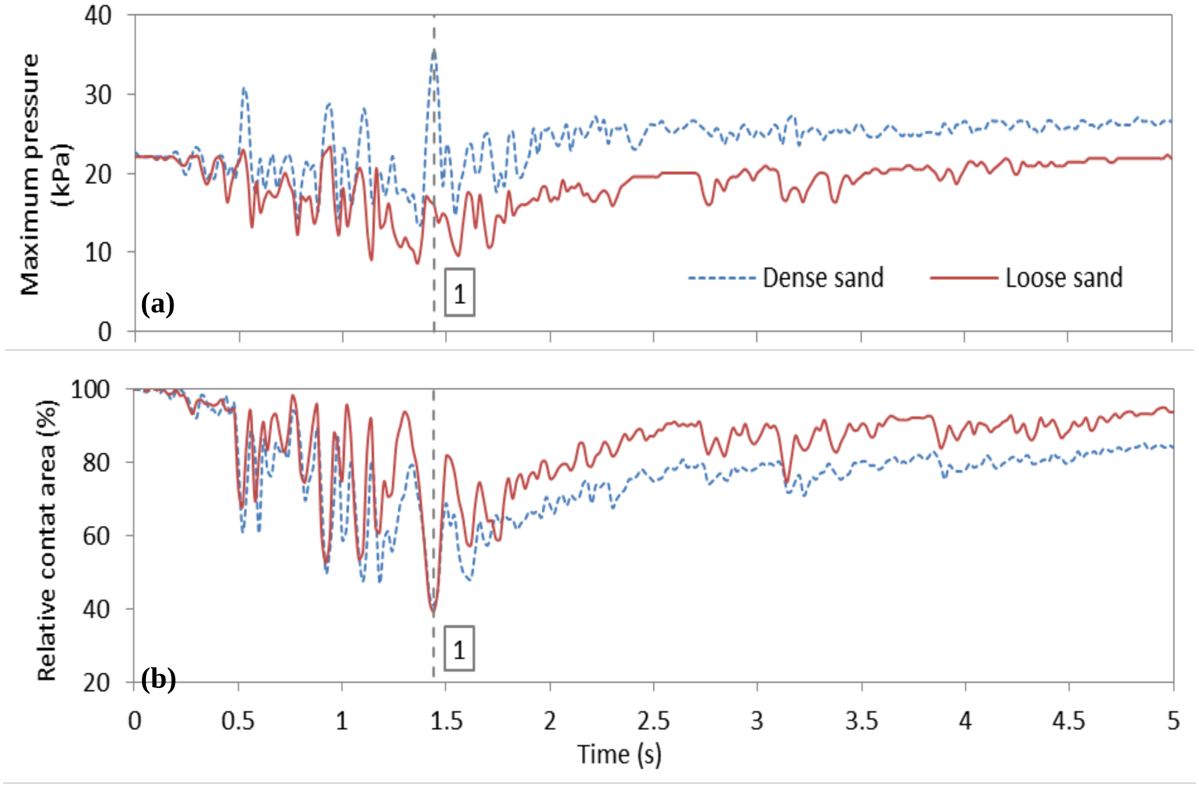

Figure 6. Pressure mat readings: (a) Maximum pressure and (b) foundation-soil contact area.

At the end of the CCCC motion for the model on dense sand, the relative contact area has decreased to 80% (Fig. 6(b)). Residual settlements of the edges of the foundation at the termination of motion are shown in Figure 10(b). It can be seen that the density of the sand significantly affects the residual displacements, both at the edges and at the centre (the mean of the edge displacements). The loss of contact was most prominent at the foundation edges. The soil -foundation relative contact area of the model on loose sand decreased to 90% at the end of the CCCC motion; while the foundation experienced a significant settlement, (14.3 mm at the centre).

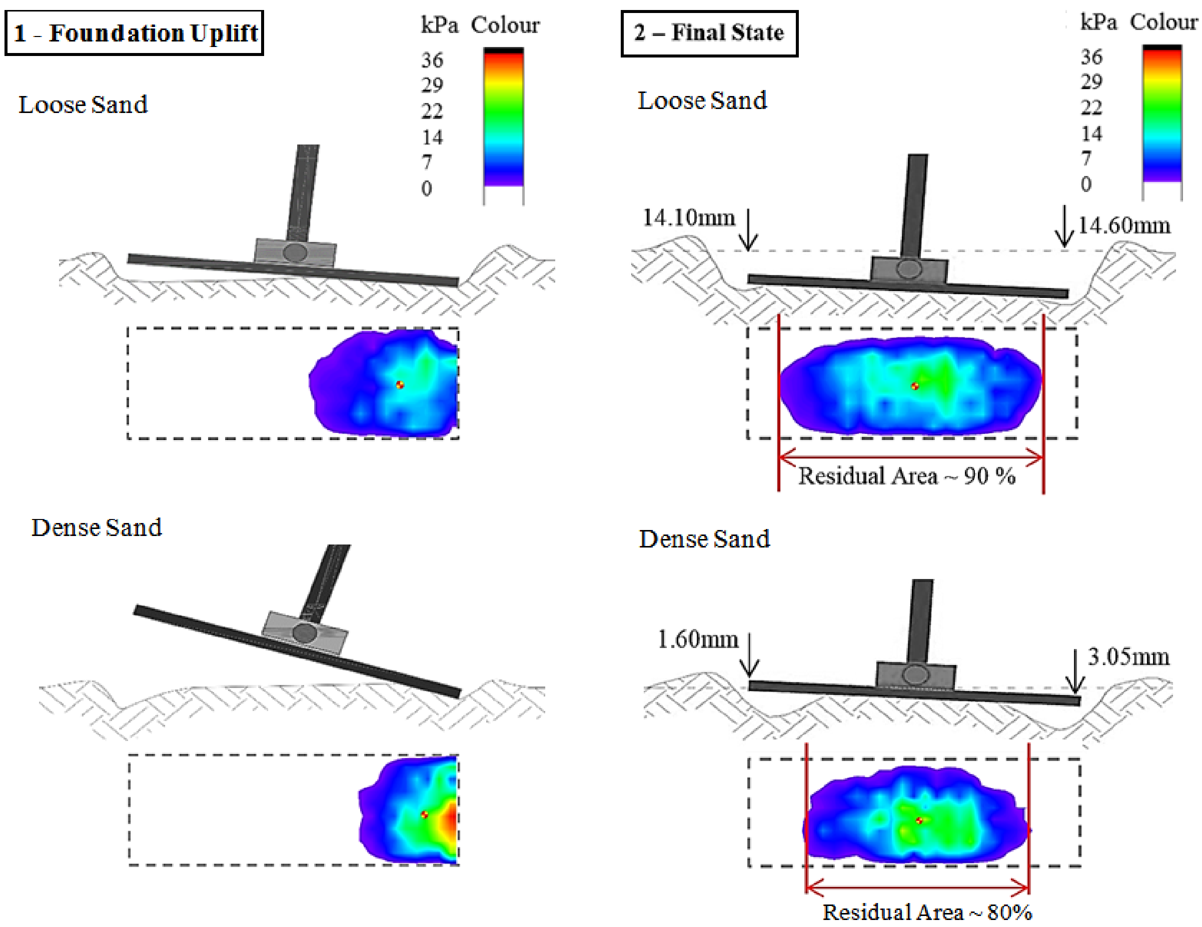

Figure 7. Foundation schematic and pressure distribution between foundation-soil interface: (1) during the pulse and (2) after shaking.

4 CONCLUSIONS

The study investigated the effects of soil density on the response of a bridge pier including soil-foundation-structure-interaction. A single-degree of freedom model was subjected to both near-fault and far-field ground motions using a shake table. A laminar box filled with sand was used to impart the seismic motion to the model in the case of SFSI investigations. The study revealed that:

- During the near-fault ground motion, the dominant frequency of the motion of the mass of the model reduces with a reduction in the relative density of the sand.
- The maximum contact pressure, which occurred during the strong acceleration pulse, of the foundation on dense sand was of the order of twice that of the loose sand. However, the total contact area remained approximately equal in both cases.
- The residual settlement of the foundation on loose sand was more than 10 times that of the foundation on dense sand.
- The maximum absolute top displacement of the model on loose sand under the CCCC motion was approximately 3 times that resulting from application of the NZS motion. For the analogous case of a foundation free to uplift on a rigid base there was little difference between the displacements. This highlights the effect of significant SFSI, as a result of a compliant sand supporting medium and an incident earthquake motion containing more long period energy.

5 ACKNOWLEDGMENTS

The research is funded by the Ministry of Business, Innovation and Employment through the Natural Hazards Research Platform under the Award UoA 3701868. The authors would like to thank the anonymous reviewer for the constructive comments that have improved the clarity of this contribution.

6 REFERENCES

Anderson, J.C. & Bertero, V.V. 1987. Uncertainties in establishing design earthquakes. *Journal of Structural Engineering*, 113(8): 1709-1724.

Bradley, B.A. 2012. Strong ground motion characteristics observed in the 4 September 2010 Darfield, New Zealand earthquake, *Soil Dynamics and Earthquake Engineering*, 42: 32-46.

Chen, Y., Chouw, N. & Larkin, T. 2013. The effect of foundation uplift and plastic yielding on induced seismic vibration of secondary structures. *New Zealand society for Earthquake Engineering annual conference, 2013, Wellington, New Zealand.*

Cheung, W.M., Qin, X., Chouw, N. Larkin, T. & Orense R. 2013. Experimental and numerical study of soil response in a laminar box. *New Zealand society for Earthquake Engineering annual conference, 2013, Wellington, New Zealand.*

Chopra, A.K. & Chatpan, C. 2001. Comparing response of SDF systems to near-fault and far-fault earthquake motions in the context of spectral regions. *Journal of Earthquake Engineering and Structural Dynamics*, 113(8): 1709-1724.

DBH 2011. *Compliance Document for the New Zealand Building Code – Clause B1 Structure*, Department of Building and Housing, Wellington, New Zealand.

Drosos, V., Georgarakos, T., Loli, M., Anastasopoulos, I., Zarzouras, O., & Gazetas, G. 2012. Soil-foundation-structure interaction with mobilization of bearing capacity: experimental study on sand, *Journal of Geotechnical and Geoenvironmental Engineering,* ASCE 2012, 138: 1369-1386.

GeoNet (2011) Strong motion FTP site, from ftp://ftp.geonet.org.nz/strong/processed /Proc/2011/02_Christchurch_mainshock_extended_pass_band

Li, B., Bi, K., Chouw, N., Butterworth, J.W. & Hao, H. 2012. Experimental investigation of spatially varying effect of ground motions on bridge pounding. *Earthquake Engineering and Structural Dynamics*, Vol 41(14), 1959-1976.

NZS 1170.5. 2004. *Structural Design Action, Part 5: Earthquake Actions*. Standards New Zealand, Wellington, New Zealand. ISBN 1-86975-018-7.

NZS 4402.4.2. 1997. *Determination of the minimum and maximum dry densities and relative density of a cohesionless soil*. Standards New Zealand, Wellington, New Zealand. ISBN 1-86975-018-5.

NZGS. 2005. *Field Description of Soil and Rock*. NZ Geotechnical Society Inc. 12-2005. Retrieved from http://www.nzgs.org/Publications/Guidelines/soil_and_rock_field_guide.pdf on 01/02/2014.

Palmer, M.C., O'Rourke, T.D., Olson, N.A., Abdoun, T., Ha, D. & O'Rourke M.J. 2009. Tactile pressure sensors for soil-structure interaction assessment. *Journal of geotechnical and geoenvironmental engineering*, 135(11): 1638-1645.

Qin,X., Chen,Y. & Chouw,N. 2013. Effect of uplift and soil non-linearity on plastic hinge development and Induced Vibrations in Structures. *Advances in Structural Engineering*, 16(1): 153-147.

Rodriguez, M. E. & Montes, R. 2000. Seismic response and damage analysis of buildings supported on flexible soils, *Earthquake Engineering and Structural Dynamics*, 29(5): 647-665.

Somerville, P. 1997. The characteristics and quantification of near-fault ground motion, *Proceedings of the FHWA/NCEER workshop on the national representation of seismic ground motion for new and existing highway facilities. Burlingame, California.*

Storie, L.B., Pender, M.J., Clifton, G.C. & Wotherspoon, L.M. 2014. Soil-foundation-structure-interaction for buildings on shallow foundations in the Christchurch earthquake. *10th US National Conference of Earthquake Engineering* 2014, Anchorage, Alaska.

Trifunac, M.D. & Todorovska, M.I. 1990. Reduction of structural damage by non-linear soil response, *Journal of Structural Engineering*, 125(1): 89-97.